Fingering patterns in the lifting flow of a confined miscible ferrofluid

Ching-Yao Chen* and S.-Y. Wu
Department of Mechanical Engineering, National Yunlin University of Science and Technology, Yunlin, Taiwan, Republic of China

José A. Miranda†
Laboratório de Física Teórica e Computacional, Departamento de Física, Universidade Federal de Pernambuco, Recife, Pernambuco 50670-901 Brazil

(Received 14 July 2006; revised manuscript received 16 November 2006; published 26 March 2007)

Miscible flow displacements of a ferrofluid droplet subjected to various magnetic field configurations and confined in a time-dependent gap Hele-Shaw cell are examined through highly accurate numerical simulations. The interplay between lifting, miscibility, and applied magnetic fields resulted in complex interfacial pattern formation. By varying the symmetry properties of the applied magnetic fields and by considering the action of Korteweg stresses, a number of interesting droplet morphologies are identified and characterized. The possibility of controlling the degree of fluid mixing and the ultimate shape of the emerging patterns by appropriately adjusting the strength of the applied magnetic fields is also discussed.

DOI: 10.1103/PhysRevE.75.036310 PACS number(s): 47.15.gp, 47.11.−j, 47.54.−r, 47.65.Cb

I. INTRODUCTION

Ferrofluids are stable colloidal suspensions of magnetic nanoparticles suspended in a nonmagnetic carrier fluid. These magnetic fluids conveniently combine the fluidity of liquids and the magnetic properties of solids, which makes them a fascinating field of research for physicists, chemists, and engineers [1,2]. One of the most useful and interesting properties of ferrofluids is their pronounced superparamagnetic behavior which allows one to manipulate their flow and interfacial behavior with external magnetic fields. Consequently, the phenomena of interfacial pattern formation in ferrofluids has received considerable attention [3–5].

One striking example of pattern-forming systems in ferrofluids is related to the famous Rosensweig instability [6,7], which leads to the development of three-dimensional (3D) stationary hexagonal array of peaks when a uniform magnetic field is applied normal to an initially flat, ferrofluid free surface. Another type of remarkable patterns is associated with the so-called labyrinthine instability [8–11], where highly branched structures are formed when a ferrofluid droplet is trapped in the effectively 2D geometry of a Hele-Shaw cell [12] under a perpendicular uniform magnetic field. More recent variations of these two classical ferrofluid instabilities revealed other extraordinary properties of these systems: (i) stable solitonlike structures are formed on the surface of a magnetic fluid in the hysteretic regime of the Rosensweig instability [13], allowing a unique soliton stabilization mechanism characterized by conservation of energy; (ii) experimental studies of the Rosensweig instability in very thin ferrofluid films reveal the rupture of the film, followed by the formation of impressive, well-ordered patterns of separated peak structures [14]; and (iii) a confined ferrofluid droplet undergoes to a sort of "phase transition" evolving smoothly to beautiful spiral patterns or suddenly morphing into amazing protozoanlike shapes, when the usual perpendicular field configuration is supplemented by a rotating magnetic field [15–17]. Other studies examined the role of the magnetic field in controlling viscosity-driven instabilities [18], centrifugally induced fingering [19,20], and stretch-flow interfacial irregularities [21,22] in thin films of ferrofluids.

Despite the rich physics and the great variety of situations explored in the study of pattern formation in ferrofluids, the large majority of such investigations deal with *immiscible* ferrofluids. So in general it is assumed that the ferrofluid does not mix with the surrounding nonmagnetic fluid, establishing a well-defined sharp interface between them which presents a nonzero surface tension. However, it is also of importance and interest to study pattern morphology when we have a *miscible* ferrofluid, where interfacial tension is negligible and diffusive effects take over.

Even though the development of the labyrinthine instability in miscible ferrofluids has been investigated by qualitative experiments [23] and preliminary theoretical models [24] for some time, only quite recently have more systematic theoretical analysis [25] and intensive computer simulations [26–30] been performed. Reference [25] carried out a linear stability analysis of the miscible labyrinthine instability in rectangular Hele-Shaw geometry and established a parallel between approaches based on Darcy's law and on the Brinkman equation. On the other hand, Refs. [26–30] employed a series of sophisticated numerical simulations which extended the study of the miscible ferrofluid problem in many different ways, considering the action of perpendicular and azimuthal magnetic fields and exploring the influence of Korteweg stresses [31–36] in radial and rotating Hele-Shaw cells of *fixed* gap width. These stresses may significantly affect the behavior of the diffuse interface, introducing surface tensionlike effects within areas of steep concentration gradients.

Very recently the miscible flow of *nonmagnetic* fluids in a time-dependent Hele-Shaw cell was investigated [37]. In such a version of the problem, the uniform lifting of the upper plate of a variable-gap Hele-Shaw cell makes the dif-

*Electronic address: chingyao@yuntech.edu.tw
†Electronic address: jme@df.ufpe.br

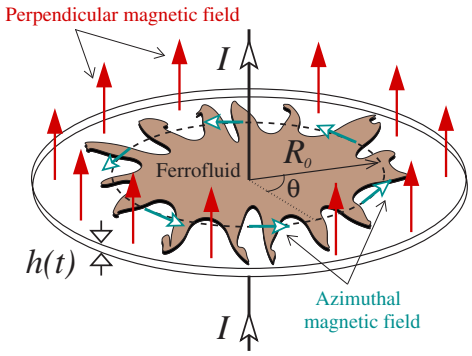

FIG. 1. (Color online) Schematic representation of the time-dependent gap Hele-Shaw cell with miscible fluids. The inner fluid is a miscible ferrofluid, and the surrounding fluid is nonmagnetic. The uniform perpendicular magnetic field and the nonuniform azimuthal magnetic field are also shown.

fuse fluid-fluid interface to move inwards, forming visually striking fingering patterns. This type of flow has been extensively studied during the last few years due to its relevance to adhesion-related problems [38–46]. In Ref. [37] the combined role played by diffusive effects, lifting rates, viscosity contrast, and Korteweg stress in determining interfacial behavior has been analyzed.

In this paper we analyze the lifting flow (*variable* gap width) situation considering that the inner fluid is both *miscible* and *magnetic* (the outer fluid is nonmagnetic), under the influence of applied magnetic fields. In this context, our aim is to consider the coupling between miscibility and magnetic effects, in both the absence and presence of Korteweg stresses, and study how they give rise to still unexplored interfacial shapes and interesting dynamical behaviors. One point of particular interest is the possibility of controlling the morphology of the patterns and the degree of mixing between the fluids by magnetic means. We also study how the interplay between magnetic forces and Korteweg stresses may interfere in such a controlled mixing and pattern-forming mechanism.

II. PHYSICAL PROBLEM AND GOVERNING EQUATIONS

The geometry of the lifting Hele-Shaw cell problem is schematically sketched in Fig. 1. We consider the miscible displacement and the development of interfacial instabilities when an initially circular ferrofluid droplet of radius R_0 and viscosity η_m is surrounded by a less viscous (nonmagnetic) fluid of viscosity η_n. The coordinate system is defined in such a way that its origin is located at the center of the droplet (which lies in the x-y plane), while the transversal gap direction is defined along the z axis. In this confined environment the flow takes place between two narrowly spaced flat plates, where the lower plate is held fixed and the upper plate is lifted at a specified rate. As in Refs. [21,22,42,43] we assume an exponentially increasing time-dependent gap width $h(t)=h_0\exp(\alpha t)$, where α is a lifting control parameter and h_0 represents the initial plate spacing.

During the lifting process we consider the action of three different magnetic field configurations: (a) *perpendicular*, when a uniform field is applied normal to the cell plates; (b) *azimuthal*, for an in-plane nonuniform field produced by a long current-carrying wire coaxial with the plates and oriented along the z axis; and (c) *crossed*, when the perpendicular and the azimuthal fields are applied simultaneously.

The dynamical evolution of the mixing interface in a time-dependent gap Hele-Shaw cell is governed by the following *gap-averaged* equations [26–30,37]:

$$\mathbf{u} = -\frac{h^2}{12\eta}\left\{\nabla[p+Q] - \nabla\cdot[\hat{\delta}(\nabla c)(\nabla c)^T] - \left[\mu_0 M_a(c)\nabla H_a + \frac{\mu_0 M_p(c)}{2\pi h}\nabla\Psi_p\right]\right\}, \tag{1}$$

$$\nabla\cdot\mathbf{u} = -\frac{\dot{h}(t)}{h(t)}, \tag{2}$$

$$\frac{\partial c}{\partial t} + \mathbf{u}\cdot\nabla c = D\nabla^2 c. \tag{3}$$

A generalized Darcy's law for miscible ferrofluids is expressed by Eq. (1) where the gap averaged fluid velocity is $\mathbf{u}$, p is the hydrodynamic pressure, η is the concentration-dependent viscosity of the mixture, and Q is the additional pressure due to the Korteweg stresses [34,36]. The gap-invariant concentration of the ferrofluid is represented by c, and $\hat{\delta}$ is the Korteweg stress coefficient. The third term between square brackets on the right-hand side of Eq. (1) represents the magnetic force contribution, which depends on the concentration-dependent magnetization of the ferrofluid in the azimuthal $M_a(c)$ and perpendicular $M_p(c)$ directions and on the gradient of the local magnetic fields. The free-space magnetic permeability is represented by μ_0.

We follow the standard approximations used in Refs. [25–30] and assume that the magnitude of the concentration-dependent magnetizations is taken as directly proportional to concentration c such that $M_a(c)=cM_{ma}$ and $M_p(c)=cM_{mp}$, where M_{ma} and M_{mp} are the corresponding constant magnetizations of the pure magnetic fluid when $c=1$. Note that the presence of a concentration-dependent magnetization in the current miscible ferrofluid case prevents one from writing the magnetic terms in Eq. (1) simply as gradients of generalized magnetic pressures, as was actually the case for immiscible ferrofluids [8–10,19,20]. Equation (2) expresses a modified incompressibility condition which accounts for the lifting of the upper plate, and the overdot denotes the total time derivative. The concentration equation is given in Eq. (3), where D is a constant diffusion coefficient. Our Darcy's law approach considers that the system remains of large aspect ratio during the entire lifting process and assumes that Taylor dispersion [47] is significant. A more detailed account about the validity and restrictions of the Darcy's law approach can be found in Refs. [37,48].

Here we would like to discuss a few important points related to the usefulness and validity of Eq. (1) when the azimuthal and perpendicular magnetic fields act simultaneously (crossed field situation). In general, if the ferrofluid magnetization function is nonlinear with the total magnetic

field, one cannot simply add the separate magnetic force components together as expressed in our generalized Darcy's law [Eq. (1)]: the magnetic fields themselves certainly obey linear superposition, but the magnetization will not necessarily do it. So it is important to clarify under what basic condition our Eq. (1) would be valid and technically correct in the crossed field case. The separation of the magnetic force as a sum of two parts (one due to the azimuthal field and the other to the perpendicular field) is possible when the magnetization is linear with the total magnetic field. Considering the linear relationship $M=\chi H$, where χ is a constant magnetic susceptibility, the magnetic body force can be written as

$$\boldsymbol{F}_m = \mu_0 M \nabla H = \mu_0 \chi H \nabla H = \mu_0 \chi \frac{1}{2} \nabla H^2, \tag{4}$$

where $M^2=M_a^2(c)+M_p^2(c)$ and $H^2=H_a^2+H_p^2$ denote the magnitudes of the magnetization and total magnetic field, respectively. Under such circumstances, Eq. (4) can be easily rewritten as

$$\boldsymbol{F}_m = \mu_0 M_a(c) \nabla H_a + \mu_0 M_p(c) \nabla H_p. \tag{5}$$

Concerning the perpendicular component of the magnetic field (H_p), we adopt an approximation which has been well used by many others in the literature (see, for instance, Refs. [1,2,8–11,25]). This approximation incorporates the "fringing fields" of a parallel-plate capacitor type of calculation for the ferrofluid droplet, which only considers the z component of the perpendicular field. Here and in Refs. [1,2,8–11,25] we assume that these fringing fields are small compared to the applied fields and include only a lowest-order contribution, so that $H_p=H_0-\partial\psi_p/\partial z$, where H_0 is the uniform perpendicular applied field and $\psi_p(x,y,z)$ is a 3D magnetic scalar potential related to the demagnetizing field contribution (or fringing field), caused by the surface magnetic dipoles. Notice that using only this perpendicular field H_p (no azimuthal component required) the magnetic droplet loses its axial symmetry and one absolutely sees the fingering (labyrinthine) instability [1,2,8–11,25]). The gap average calculation of Eq. (5), $\int_0^h \boldsymbol{F}_m dz/h$, leads exactly to the magnetic contribution shown in our Darcy law [Eq. (1)], where $\Psi_p(x,y,z=h)$ is the value of $\psi_p(x,y,z)$ on the upper Hele-Shaw plate. This explains more quantitatively why we can take the z-averaged magnetic body force presented in Eq. (1) as simply the sum of two independent parts.

Experimental measurements of the magnetization of miscible ferrofluids as a function of magnetic field strength for various concentrations of magnetic particles [49] demonstrate a typical Langevin function behavior: a nearly linear relationship at smaller field strengths and then a saturated magnetization. The concentration of magnetic particles does not alter the features of this dependence, but only affects the strength of the magnetization. Furthermore, the strength of saturated magnetizations is proportional to the concentration. On this basis, our theoretical approach assumes that the magnetization is in fact linear with the magnetic field, as long as the field strength is not too intense. This simplifying assumption is probably not the most general one; however, it is certainly valid as a first theoretical approximation, which is still amenable for the numerical modeling of the system under the crossed field situation.

For the sake of clarity, we also call the reader's attention to the notation used for the magnetizations M_{ma} and M_{mp} when the fields act separately or simultaneously. Within the scope of our theoretical approach, M_{mp} (M_{ma}) is the magnetization component related to the repelling (attracting) magnetic forces associated with the perpendicular (azimuthal) field. In a purely perpendicular (azimuthal) field situation, M_{mp} (M_{ma}) is simply the corresponding magnetization due to the sole action of the perpendicular (azimuthal) field. Of course, in the situation of a crossed magnetic field, the values of these two magnetization components are not necessarily the values obtained from the above single-field conditions. Instead, they represent the actual values that are induced by the total field.

The local magnetic field can include contributions from the applied field as well as the demagnetizing field [1,2]. We consider only the lowest-order effect of the magnetic interactions that would result in fluid motion. The in-plane azimuthal magnetic field is nonuniform, such that it naturally possesses a radial gradient. Thus, in the azimuthal field configuration the demagnetizing effects are negligible and we can consider the sole action of the applied magnetic field [19]:

$$\mathbf{H}_a = \frac{I}{2\pi r} \hat{\mathbf{e}}_\theta, \tag{6}$$

where I represents the electric current passing through the current carrying-wire , r is the distance from the wire, and $\hat{\mathbf{e}}_\theta$ is a unit vector in the azimuthal direction. This field produces a magnetic force directed radially inward, which tends to move the miscible ferrofluid toward the current-carrying wire (regions of higher magnetic field), favoring an interface stabilization.

In the perpendicular case the situation is a bit different: the local field differs from the externally applied uniform field by a droplet-shape-dependent demagnetizing magnetic field [8–10]. This configuration is equivalent to a uniformly charged parallel-plate capacitor, where spatially varying fringe fields arise. Under such circumstances the demagnetized field can be conveniently written in terms of a scalar potential [25–27]

$$\Psi_p = -M_{mp}\mathcal{J}, \quad \mathcal{J} = \int c\left[\frac{1}{d} - \frac{1}{\sqrt{d^2+h^2}}\right] d\mathcal{S}', \tag{7}$$

where d is the magnitude of the difference vector $\mathbf{d}=\mathbf{r}-\mathbf{r}'$. The unprimed coordinates denote arbitrary points in the Hele-Shaw cell, the primed coordinates are integration variables within the magnetic fluid domain, and $d\mathcal{S}'$ represents the infinitesimal-area element of the effectively 2D ferrofluid droplet. The perpendicular field tends to align the tiny magnetic moments of the miscible ferrolfuid in a direction normal to the Hele-Shaw cell plates, so that they repel each other and the mixing interface becomes unstable. It is worth noting that, in contrast to the corresponding immiscible fer-

rofluid situation, here the resulting flow is in general not potential owing to the inhomogeneity of c.

The viscosity variations of the mixture are assumed as [50,51]

$$\eta(c) = \eta_m \exp[\mathcal{R}(1-c)], \tag{8}$$

where $\mathcal{R}=\ln(\eta_n/\eta_m)$ is a logarithmic viscosity ratio. In order to render the governing equations dimensionless, the radius of the initial circular droplet R_0 is used as the characteristic length scale. We further scale the viscosity with η_m and time with $1/\alpha$. In conjunction with characteristic velocity αR_0 and pressure $12\eta_m\alpha$, dimensionless governing equations are obtained:

$$\mathbf{u} = -\frac{e^{2t}}{\hat{\eta}}\left\{\hat{h}_0^2\nabla[p+Q] - \nabla\cdot[\delta(\nabla c)(\nabla c)^T] - \left[N_a c\nabla\left(\frac{1}{r}\right) - e^{-t}N_p c\nabla\mathcal{J}\right]\right\}, \tag{9}$$

$$\nabla\cdot\mathbf{u} = -1, \tag{10}$$

$$\frac{\partial c}{\partial t} + \mathbf{u}\cdot\nabla c = \frac{1}{\mathrm{Pe}}\nabla^2 c, \tag{11}$$

where $\hat{\eta}=\eta(c)/\eta_m$. Dimensionless parameters, such as the Péclet number Pe, the viscosity contrast A, the perpendicular and azimuthal field strengths N_p and N_a, the Korteweg constant δ, and the initial gap width $\hat{h}_0$, are defined as

$$\mathrm{Pe} = \frac{\alpha R_0^2}{D}, \quad A = \frac{\eta_m-\eta_n}{\eta_m+\eta_n}, \quad N_a = \frac{\mu_0 M_{ma} I h_0^2}{24\pi\eta_m\alpha R_0^3},$$

$$N_p = \frac{\mu_0 M_{mp}^2 h_0}{24\pi\eta_m\alpha R_0}, \quad \delta = \frac{\hat{\delta}h_0^2}{12\eta_m\alpha R_0^4}, \quad \hat{h}_0 = \frac{h_0}{R_0}.$$

From now on, we work with the dimensionless version of the equations.

The velocity is split into a divergence-free component $\mathbf{u}_f$, which is the velocity of the constant-gap-spacing case, and an axisymmetric divergent radial velocity $\mathbf{u}_d=\mathbf{u}_d(r)$ caused by the gap variation, so that $\mathbf{u}=\mathbf{u}_f+\mathbf{u}_d$ and

$$\nabla\cdot\mathbf{u}_f = 0, \tag{12}$$

$$\nabla\cdot\mathbf{u}_d = -1. \tag{13}$$

The divergent radial velocity is obtained directly from Eq. (13) as $\mathbf{u}_d=-\mathbf{r}/2$, which is a potential field. On the other hand, by rewriting Eq. (9) in a stream function ϕ and vorticity ω formulation, the divergence-free component $\mathbf{u}_f$ can be obtained by solving the equations [34,51,52]

$$u_f = \frac{\partial\phi}{\partial y}, \quad v_f = -\frac{\partial\phi}{\partial x}, \tag{14}$$

$$\nabla^2\phi = -\omega, \tag{15}$$

$$\omega = -\mathcal{R}\left[u\frac{\partial c}{\partial y} - v\frac{\partial c}{\partial x}\right] - \frac{e^t N_p}{\hat{\eta}}\left[\frac{\partial c}{\partial x}\frac{\partial\mathcal{J}}{\partial y} - \frac{\partial c}{\partial y}\frac{\partial\mathcal{J}}{\partial x}\right] - \frac{e^{2t}N_a}{\hat{\eta}r^3}\left[y\frac{\partial c}{\partial x} - x\frac{\partial c}{\partial y}\right] - \frac{e^{2t}\delta}{\hat{\eta}}\left[\frac{\partial c}{\partial x}\left(\frac{\partial^3 c}{\partial x^2\,\partial y} + \frac{\partial^3 c}{\partial y^3}\right) - \frac{\partial c}{\partial y}\left(\frac{\partial^3 c}{\partial x\,\partial y^2} + \frac{\partial^3 c}{\partial x^3}\right)\right]. \tag{16}$$

Since there is no net flux of the divergence-free flow through the computational domain, we therefore can arbitrarily take vanishing values of a divergent-free stream function at the boundaries. Therefore, the choice of computational domain is arbitrary as long as the domain contains the whole droplet. Of course, the divergent radial component is still present within the entire computational domain. We choose the boundaries to vary between $+4/3$ and $-4/3$ in both the x and y directions. Under such circumstances, the boundary conditions are prescribed as follows:

$$x = \pm\frac{4}{3}: \frac{\partial\phi}{\partial x} = 0, \quad \frac{\partial c}{\partial x} = 0, \tag{17}$$

$$y = \pm\frac{4}{3}: \phi = 0, \quad \frac{\partial c}{\partial y} = 0. \tag{18}$$

The implementation of vanishing gradients of ϕ at x-directional boundaries allows the application of a highly accurate spectral method, which is essential to reproduce extremely fine structures. The stream function, Eq. (15), is solved by a pseudospectral method, and a Galerkin-type discretization of cosine expansion is employed in the x direction. In the y direction discretization is accomplished by sixth-order compact finite differences. In addition, the vorticity equation (16) is evaluated by sixth-order compact finite-difference schemes. A third-order Runge-Kutta procedure on time and spatial sixth-order compact finite-difference schemes are employed to solve the concentration, Eq. (11), and advanced in time. The numerical code has been successfully used for miscible flow in other geometries [27,36,51,53] and is quantitatively validated by comparing the growth rates with the values obtained from the linear stability theory in a plane front. More details on the implementation and quantitative validation of these schemes are provided by Refs. [27,52,54].

At this point we believe some clarifications about the discretization schemes along the x-y directions and a more detailed justification of the particular choice of boundary conditions [Eqs. (17) and (18)] are necessary. Ideally speaking, by considering the circular geometry and symmetric nature of the physical problem under study, it may seem obvious that the most appropriate theoretical description would obligatorily involve the use of a polar coordinate system. However, this is not exactly the case when an accurate numerical description of the problem needs to be implemented. In order to successfully generate the extremely fine and intricate fingering structures emerging in the lifting flow of a miscible ferrofluid, a highly accurate numerical scheme is required. To accomplish this task, spectral methods associated with discretizations by high-order compact finite-

difference schemes are a very useful tool. In practice, the use of such spectral methods, which require periodic boundaries in one direction, and of compact finite difference schemes, which perform better in a uniform grid, impose serious limitations on the implementation of a numerical code based on polar coordinates. In this sense, the ability of generating extremely fine patterning structures is somewhat incompatible (or at least much more difficult) with the eventual choice of polar coordinates. This is why we have adopted a rectangular coordinate system to describe the current lifting flow situation. In addition, the implementation of the mentioned highly accurate numerical schemes can avoid significant numerical artificial diffusion often associated with lower-order schemes, making their use essential for reproducing the extremely fine and complex structures in the present situation.

Regarding the particular choice of the boundary conditions [Eqs. (17) and (18)], as mentioned above, they consider that the stream function is zero for all boundaries. Nevertheless, to apply the spectral method along the x direction, we need to modify the boundary condition as $\partial\phi/\partial x=0$. The validity of these modified conditions is achieved by carefully keeping the mixing interface far away from the boundaries at all times, so that the vorticity and stream function induced by the concentration gradients are vanishingly small and negligible near the boundaries. All this is confirmed by the nearly zero values of the stream function obtained from the actual numerical output data. With respect to the nonsymmetric nature of the boundaries, eventual problems are well resolved if the values of the field variables (such as ϕ and c) are very close to zero near the boundaries, which are exactly the situations described in our simulations. Since all these values are effectively zero, all the derivatives would also be zero and therefore satisfy the symmetric conditions locally.

Therefore, a description of the domain in x-y (Cartesian) coordinates is essential for the applicability of the present highly accurate numerical scheme. Under such circumstances, we realize that a certain degree of artificial numerical features are inevitable. This is especially noticeable in situations of stronger magnetic field strengths at later time stages, when the curvature of the diffusing interface is significant. For the sake of correctness and considering the range of validity and accuracy of our numerical approach, we only consider patterns which are not strongly and artificially influenced by the numerical procedure we used. Despite the possible limitations and the justified concerns regarding the proper grid coordinates, we stress that the numerical scheme we utilize in this work has been successfully applied to describe other problems dealing with a miscible circular droplet in confined geometry. The most obvious successes are the excellent results recently obtained in Refs. [37,48] which describe the miscible displacement of originally circular (nonmagnetic) droplets in lifting and rotating Hele-Shaw flows. By applying the same mathematical model we use here, we have obtained excellent agreements (both qualitatively and quantitatively) with existing experiments and other numerical approaches describing immiscible flow in such radially symmetric systems. All these findings support the applicability, reliability, and general appropriateness of our numerical approach.

III. RESULTS AND DISCUSSION

We examine the effects of the applied magnetic fields on the morphology of the patterns formed during the lifting flow. Throughout this work we consider that the ferrofluid is much more viscous than the invading nonmagnetic fluid, so that the viscosity contrast is very high ($A=0.905$) and the Saffman-Taylor (viscosity-driven) instability is maximized. Moreover, since we are primarily interested in the interplay between magnetic and miscibility effects, the Péclet number ($\mathrm{Pe}=2.0\times10^{3}$) and the initial gap spacing ($\hat{h}_0=0.01$) are kept fixed, while the Korteweg stress parameter δ and the magnetic field strengths N_a and N_p are allowed to vary.

We emphasize that the initial conditions are exactly the same for all patterns simulated in this work. These initial conditions assume a circular shape bounded by a steep concentration gradient in a form of error function radially. The radial profile of the error function has an inflection point (0.5 concentration) located at a unit radial distance from the origin. To break the unphysical artificial symmetry, a small magnitude of random noises is applied to the positions of 0.5 concentration. It is known that the fingering patterns of miscible interfaces could depend on the initial condition [25] since the concentration gradient is the main source of instabilities. Throughout all the simulations presented in this work, we apply the same profile of the error function, as well as an identical set of random noises in order to eliminate the sensitivity due to such effects.

A. Combined influence of magnetic fields and Korteweg stresses

We begin our investigation by considering the purely miscible case in which the Korteweg stress is zero ($\delta=0$). Figure 2 illustrates the patterns obtained at time $t=1.25$ when (a) the lifting occurs in the absence of magnetic field, (b) only the perpendicular magnetic field is applied ($N_p=10^{-1}$), (c) only the azimuthal field is present ($N_a=3.0\times10^{-2}$), and (d) both magnetic fields act simultaneously ($N_p=10^{-1}$ and $N_a=3.0\times10^{-2}$). When the fields are both zero [Fig. 2(a)] we obtain the typical morphological structure recently obtained in Ref. [37] for the lifting flow of nonmagnetic fluids in Hele-Shaw cells. Basically, the fingering instabilities are viscosity induced and produced by the inward motion of the less viscous fingers of the outer fluid penetrating the more viscous ferrofluid. Moreover, due to the miscible nature of the fluids, the interface is further destabilized. Therefore, even in the absence of applied magnetic fields, the resulting pattern is considerably complex, showing a disordered array of fingers presenting various lengths and widths.

When a perpendicular field is applied [Fig. 2(b)] the emerging pattern is quite intricate. Due to the magnetic repulsion induced by the perpendicular field, the outward moving fingers of the ferrofluid tend to ramify even further and become very thin, while the inward moving fingers are not as wide as the one shown in the absence of magnetic fields [Fig. 2(a)]. The combination of lifting, miscibility, and perpendicular field produces a unique set of finely branched structures, where fingers split at their tips and eventually merge.

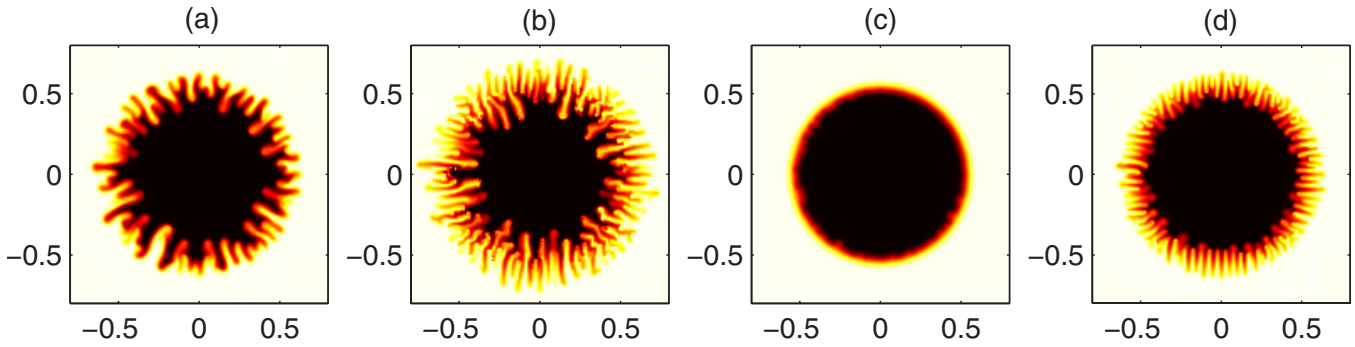

FIG. 2. (Color online) Concentration images at time $t=1.25$ and $\delta=0$ for (a) $N_p=0$, $N_a=0$; (b) $N_p=10^{-1}$, $N_a=0$; (c) $N_p=0$, $N_a=3.0\times10^{-2}$; and (d) $N_p=10^{-1}$, $N_a=3.0\times10^{-2}$.

As a result, the mixing between the fluids would be favored under perpendicular field circumstances.

The opposite effect is shown in Fig. 2(c) where only an azimuthal magnetic field is present: due to a radial field gradient, the interface is stabilized and the development of fingers (both inward and outward) is significantly inhibited. Consequently, the whole ferrofluid droplet is firmly kept around the center of the Hele-Shaw cell, preventing the penetration of the outer fluid. Thus, the mixing layer is restricted to the border of the contracting droplet. In contrast to the perpendicular field case, here the azimuthal magnetic field acts to restrain fluid mixing. Despite the effects of lifting and miscibility, by applying an azimuthal field one can maintain the contracting droplet fairly circular during the whole lifting process.

One last pattern is depicted in Fig. 2(d), where both fields (perpendicular and azimuthal) are nonzero and applied at the same time. The competition between the two fields is evident: the azimuthal field tries to preserve the circularity of the original droplet, while the perpendicular field tends to spread it out. Since the azimuthal field is much stronger near the center of the droplet, it is also clear that the destabilizing effect of the perpendicular field is more effective at the droplet boundary. It is also worth noting that the outward-moving fingers are not as ramified as the ones shown in Fig. 2(b) and now present a peculiar tendency to align along the radial direction. More details about this alignment and other aspects of the crossed field configuration will be discussed in Sec. III B. From the analysis of Figs. 2(a)–2(d) one general conclusion can be reached: despite the miscible character of the fluids and the inherent destabilizing nature of the lifting, the degree of miscibility between the fluids and the strength and complexity of the interfacial patterns can be appropriately controlled by external magnetic fields.

It is also of interest to study the possibility of reintroducing surface-tension-like effects into the miscible lifting flow, under the presence of applied magnetic fields. This can be done by considering the action of Korteweg stresses. More than a century after the seminal work by Korteweg [31], the concept of an effective surface tension (or Korteweg stress) in a miscible fluid-fluid interface is not yet completely understood. While a first-principles derivation for the action of such stresses is not yet available, there exist interesting and useful theoretical proposals in the literature for their mathematical formulation, mainly by Joseph and co-workers [32–35]. With respect to miscible displacements in Hele-Shaw cells, Hu and Joseph [34] pointed out that the Korteweg constant has to be negative in order to avoid the Hadamard instability, or otherwise a mathematical ill-posedness of the problem would arise. Their claim has been repeatedly supported by a number of intensive numerical simulations of miscible flows in Hele-Shaw cells [26–29,36,37,48], where the effects of negative Korteweg constants lead to great similarities (both qualitative and quantitative) between the simulated miscible patterns and their corresponding immiscible counterparts.

In this work, we have also performed a few numerical tests, imposing a positive sign for the Korteweg constant: our results show diffusing interfaces that are increasingly unstable for larger, positive Korteweg constants, a behavior which is inconsistent with the stabilizing nature of a surface tensionlike quantity. Based on the above information, only negative values of the Korteweg constants are used in this work in order to consistently associate the Korteweg stress with the usual surface tension effects existing between immiscible fluids. However, we would like to reiterate that the present study is mostly based on the well-established, but purely theoretical models mentioned above, where under the conditions of negative Korteweg constant, the stress acts similar to the immiscible surface tension. As to the actual sign of the Korteweg constant for certain fluid materials, in principle one should not exclude the possibility of the existence of a positive Korteweg constant for some certain compositions of fluids, as reported in Gazeau *et al.* in their experimental study of some types of magnetic colloids [55].

The combined influence of magnetic effects and Korteweg stresses is illustrated in Fig. 3. Now, $\delta=-5.0\times10^{-7}$ but all the remaining physical patterns are the same as those used in Fig. 2. We contrast the nonzero δ patterns shown in Fig. 3 with the ones depicted in Fig. 2 when $\delta=0$. By comparing the patterns obtained when there is no applied fields [Figs. 2(a) and 3(a)], an immediate conclusion is that the Korteweg stress acts quite similarly to the usual surface tension of immiscible flows, in the sense that it induces a general stabilization of the pattern (less rigorous fingering), reducing the number of fingers and increasing their typical widths. Incidentally, the morphological structure shown in Fig. 3(a) does resemble the ones normally obtained in experiments [39,40,45,46] for immiscible flow of nonmagnetic fluids in lifting Hele-Shaw cells.

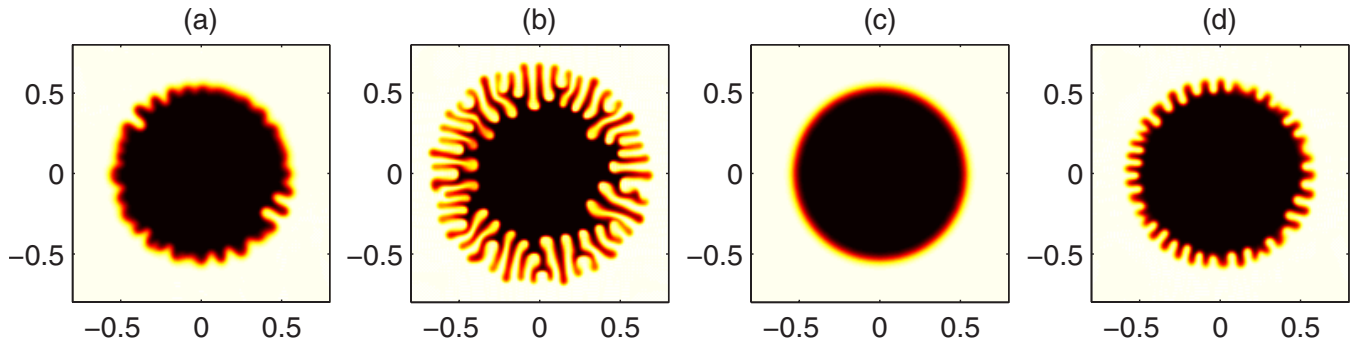

FIG. 3. (Color online) Concentration images at time $t=1.25$ and $\delta=-5.0\times10^{-7}$ for (a) $N_p=0$, $N_a=0$; (b) $N_p=10^{-1}$, $N_a=0$; (c) $N_p=0$, $N_a=3.0\times10^{-2}$; and (d) $N_p=10^{-1}$, $N_a=3.0\times10^{-2}$.

The situation is much more interesting when external magnetic fields are applied [Figs. 3(b)–3(d)]. In terms of magnetic effects, even though the azimuthal field situation [Fig. 3(c)] is not much different from the equivalent case without Korteweg stresses [Fig. 2(c)], more dramatic changes are observed for the perpendicular [Fig. 3(b)] and crossed [Fig. 3(d)] field cases. In the perpendicular field case, the introduction of Korteweg stress creates patterns that present a much closer similarity with the usual labyrinthine structures revealed by immiscible ferrofluids in *fixed*-gap Hele-Shaw cells [8–11]. However, in contrast to their immiscible counterparts, the bifurcating (forklike) structures of Fig. 3(b) arise at the perimeter of the droplet, keeping its internal region reasonably preserved.

The crossed field pattern [Fig. 3(d)] is also considerably different from the one illustrated in Fig. 2(d). It clearly displays a much more regular array of thicker fingers. Despite the action of the perpendicular field, note that these fingers do not tend to bifurcate. However, as was also the case in Fig. 2(d), the fingers in Fig. 3(d) are arranged more or less along the radial direction. The existence of such a regular distribution of easily countable fingers in the crossed field configuration when $\delta\neq0$ suggests a sort of "finger selection mechanism," in the sense that by applying both fields together one would gain greater control over the system, possibly providing a predictable way to obtain patterns in lifting Hele-Shaw flow. Further discussion about this point is presented in Sec. III B.

An alternative account of the magnitudes of the fingering instabilities can be determined by the growth of a characteristic quantity related to the perimeter of the interface, the so-called normalized interfacial length [36,51,53]

$$L_n=\frac{1}{2\pi e^{-t/2}}\int_S\sqrt{\left(\frac{\partial c}{\partial x}\right)^2+\left(\frac{\partial c}{\partial y}\right)^2}\,dxdy, \tag{19}$$

where S is the entire computational domain. This quantity expresses the ratio of the length of the diffuse interface to the perimeter of a circular interface having the same area.

Figure 4 depicts the time evolution of L_n for the applied magnitudes used in Figs. 2 and 3 for (a) $\delta=0$ and (b) $\delta=-5.0\times10^{-7}$. Evidently, the presence of Korteweg stresses tends to stabilize the diffuse interface. This can be verified by noting that the onset times for triggering the fingering instabilities (time for which L_n starts to grow) are larger in (b). It is also observed, both in (a) and (b), that once the instability starts, L_n keeps growing. However, the way L_n grows depends on whether the Korteweg stresses are present or not. For instance, if $N_p\neq0$, the growth of L_n in (a) presents a sort of "plateau," which is absent in (b). Due to the lack of a surface-tension-like constraint in (a), the diffusive effects are much stronger than in (b). Such strong diffusive effects lead to the slower growth of L_n in (a), justifying the existence of the plateaus. Of course, significant growth will pick up again (after the plateau is established), once increments of the perpendicular field (which are stronger at later times) overcome the diffusive effects. The stabilizing effects originated from the azimuthal field are also easily identified in Fig. 4, making L_n almost unchanged as time progresses.

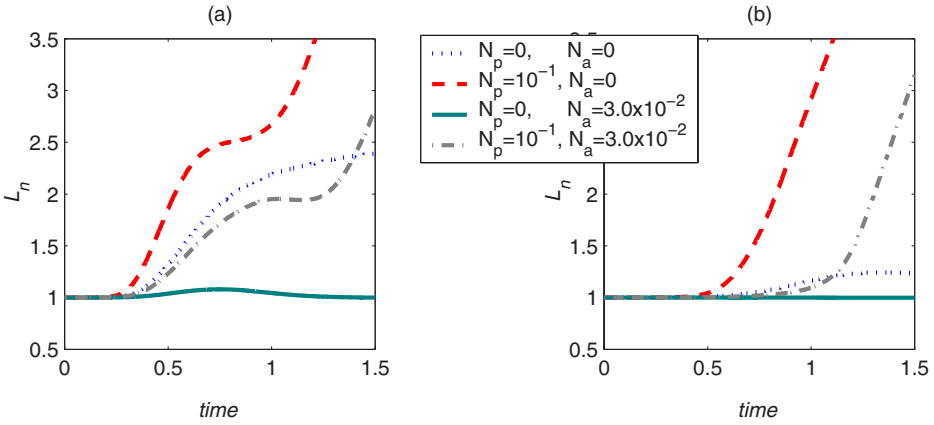

FIG. 4. (Color online) Time evolution of the normalized interfacial length L_n for various combinations of the applied magnetic fields and for (a) $\delta=0$ and (b) $\delta=-5.0\times10^{-7}$.

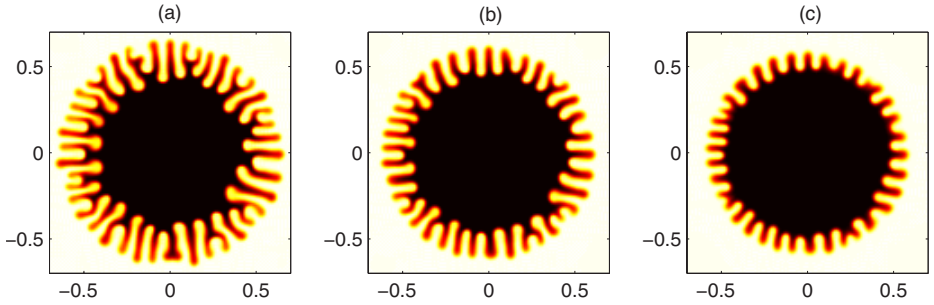

FIG. 5. (Color online) Concentration images at time $t=1.3$, $\delta=-5.0\times10^{-7}$, for a fixed $N_p=10^{-1}$ and three increasing values of the azimuthal field parameter: (a) $N_a=10^{-2}$, (b) $N_a=2.0\times10^{-2}$, and (c) $N_a=3.0\times10^{-2}$.

B. Further discussion about the crossed field situation

During the lifting process, the interfacial instability is determined by several contributions: the lifting speed (Pe), the viscosity contrast (A), the effective surface tension (Korteweg stress δ), and finally by the perpendicular (N_p) and azimuthal (N_a) field strengths. We have verified that higher Pe, A, or N_p leads to more vigorous fingering, while larger δ or N_a stabilizes the interface. However, we point out that the magnetic fields act quite differently as time evolves. The destabilizing effects of a perpendicular field are induced by dipolar repulsion, expressed as a considerably complicated scalar potential Ψ_p [see Eq. (7)]. This potential depends on the gap width of the Hele-Shaw cell. For a given value of N_p, the destabilizing effects would be more significant at later time stages when the gap width becomes wider. On the other hand, the azimuthal field presents a much simpler functional form, being proportional to the inverse of the radial distance [see Eq. (6)]. So at a later time, when the interface shrinks to a shorter radius, the stabilizing effect of N_a is indeed more significant. We conclude that, as the plates are separated further, an increasingly larger competition between these two magnetic fields should be expected. Considering all these facts, the pattern formation in a crossed field situation deserves further investigation.

The crossed field patterns for increasingly larger azimuthal field strengths ($N_a=10^{-2}$, 2.0×10^{-2}, and 3.0×10^{-2}) at a constant value of $N_p=10^{-1}$, $\delta=-5.0\times10^{-7}$, and $t=1.3$ are illustrated in Fig. 5. Depending on the strength of the azimuthal field, we see that the resulting patterns can be quite different. While there is plenty of fingering and ramification for lower N_a [Fig. 5(a)], the branching tends to disappear as N_a is increased [Figs. 5(b) and 5(c)]. This is expected, since the azimuthal field is stabilizing. However, what is not so expected is the way the fingers arrange themselves as N_a assumes larger values: in addition to the interface stabilization, the combined action of perpendicular and azimuthal fields tends to induce an ordered set of fingers which tend to align along the radial direction. This last effect is illustrated in Fig. 5(c). The azimuthal field is the major responsible for this behavior, while the perpendicular field ensures the very existence of the fingers, preventing the droplet from becoming a perfect circle. Of course, the absence of finger tip bifurcation and the production of fairly straight, well-defined fingering structures in Fig. 5(c) results in a situation in which a specific number of fingers could be selected. This suggests an interesting controlling mechanism for predicting the final number and the ultimate shape of the resulting fingers under crossed field circumstances. We have also verified the development of a similar kind of ordered patterns for many other simulations which use a variety of values for the physical parameters involved. We emphasize that in plotting Fig. 5 we use sufficiently low values for both the time taken and the azimuthal field parameters N_a so that any effects supposedly related to the numerical grid are minimized. Within this context and as already discussed in detail at the end of Sec. II, any of the relevant features revealed by the patterns presented here cannot be attributed to numerical artifacts.

The key point to obtain the selectivity exemplified in Fig. 5 is to have separate control over the stabilizing (azimuthal field) and destabilizing (perpendicular field) components of the crossed magnetic field. We stress that this selectivity does not take place when only one of the fields is present. For the sole action of the perpendicular field it is well known that the labyrinthine instability depends critically on the magnetic field ramp rate and also on the initial state of the droplet [9,10], frustrating any attempt to predict the final number of fingers. On the other hand, the isolated action of larger azimuthal fields would eventually stabilize the interface [19,20], producing a final pattern without any fingers (perfect circle). However, the simultaneous action of both azimuthal and perpendicular fields seems to provide a more predictable way to obtain patterns (generating a sort of "mode-selection mechanism") even under the complicated circumstances of viscous flow in lifting Hele-Shaw cells.

It is worth noting that a similar controlling mechanism has been very recently identified in Ref. [56] for the case in which the confined ferrofluid does not mix with the outer nonmagnetic fluid. Their numerical simulations [56] (based on conformal mapping techniques) for *immiscible* ferrofluids in *fixed*-gap Hele-Shaw cells have demonstrated that the action of a crossed magnetic field also leads to the formation of regular structures, presenting radially oriented fingers. Their analytical and numerical results strongly support the existence of a mode-selection mechanism in which the crossed magnetic fields can be specifically tuned so that any particular mode can be driven as the only unstable one. Despite the more complex nature of our present system (which considers the interplay between magnetic and lifting forces, under miscible circumstances), the independent observation (using a completely different numerical approach) of a similar mode-selection mechanism in Ref. [56] is certainly reassuring, indicating that the selection process and the general shape of the resulting patterns are not determined by any particular numerical artifact. This serves to substantiate our current findings, also indicating the effectiveness of the numerical scheme presented here for describing the miscible case.

IV. CONCLUDING REMARKS

In this work we presented accurate numerical simulations describing the formation of complicated fingering patterns when a miscible ferrofluid droplet is stretched in a lifting Hele-Shaw cell, subjected to different magnetic field configurations. We studied the development of the patterns under the separated or combined action of perpendicular and azimuthal magnetic fields. The perpendicular field is destabilizing and tends to create highly branched patterns. On the other hand, the azimuthal field acts to stabilize the contracting diffuse interface, restraining the development of interfacial fingering structures. Because of a continuous widening of the Hele-Shaw cell gap width, the diffusing interface shrinks and the strength of the magnetic effects become even more significant as the lifting progresses. These magnetic effects are investigated under purely miscible situations (complete absence of surface tension) and also by introducing an effective surface tension into the miscible system (the so-called Korteweg stresses). By considering the action of all these effects we were able to identify and characterize a number of interesting ferrofluid droplet morphologies.

We have also examined the situation in which the lifting flow occurs under the simultaneous influence of both azimuthal and perpendicular magnetic fields (crossed field situation). In addition to providing appealing interfacial patterns, the crossed field situation introduces a suggestive mechanism for finger selection in this system. So despite all intrinsic complications related to lifting and mixing, by properly tuning the values of the applied magnetic fields, one could select patterns of a given shape and numbers of fingers. This crossed field mechanism indicates the possibility of controlling the degree of miscibility between the fluids.

As a final note, we point out that the magnetically controlled mechanism described in this work can also be of interest and useful for related problems in adhesion science. There is recent evidence [40,45,46,57] that the presence of the fingering instability in lifting flow may influence the adhesion between separating plates. A study performed in Ref. [57] has indicated that the adhesiveness of a confined nonmagnetic and immiscible fluid is strongly reduced (decrease of 50% relative to the case with no fingering). In other related investigations [40,45,46] this reduction in adhesion is comparatively less intense, but still present notably for small initial plate separations. Therefore, the possibility of controlling fingering instabilities in lifting flows we presented here may offer a promising alternative to regulate adhesion via magnetic means. In addition, the consideration of adhesion-related problems involving miscible fluids seems to be another topic of interest.

ACKNOWLEDGMENTS

J.A.M. thanks CNPq (Brazilian Research Council) for financial support of this research through the CNPq/FAPESQ Pronex program and CNPq program "Instituto do Milênio de Fluidos Complexos" Contract No. 420082/2005-0. C.-Y.C. thanks the National Science Council of the Republic of China for financial support of this research through Grant No. NSC 93-2212-E-224-006. We gratefully acknowledge helpful discussions with David Jackson.

[1] R. E. Rosensweig, *Ferrohydrodynamics* (Cambridge University Press, Cambridge, England, 1985), and references therein.
[2] E. Blums, A. Cebers, and M. M. Maiorov, *Magnetic Fluids* (de Gruyter, New York, 1997), and references therein.
[3] J.-C. Bacri, R. Perzynski, and D. Salin, Endeavour **12**, 76 (1988).
[4] F. Elias, C. Flament, J.-C. Bacri, and S. Neveu, J. Phys. I **7**, 711 (1997).
[5] C. Rinaldi, A. Chaves, S. Elborai, X. He, and M. Zahn, Curr. Opin. Colloid Interface Sci. **10**, 141 (2005).
[6] M. D. Cowley and R. E. Rosensweig, J. Fluid Mech. **30**, 671 (1967).
[7] R. Friedrichs and A. Engel, Phys. Rev. E **64**, 021406 (2001).
[8] A. O. Tsebers and M. M. Maiorov, Magnetohydrodynamics (N.Y.) **16**, 21 (1980).
[9] S. A. Langer, R. E. Goldstein, and D. P. Jackson, Phys. Rev. A **46**, 4894 (1992).
[10] D. P. Jackson, R. E. Goldstein, and A. O. Cebers, Phys. Rev. E **50**, 298 (1994).
[11] G. Pacitto, C. Flament, J.-C. Bacri, and M. Widom, Phys. Rev. E **62**, 7941 (2000).
[12] P. G. Saffman and G. I. Taylor, Proc. R. Soc. London, Ser. A **245**, 312 (1958).
[13] R. Richter and I. V. Barashenkov, Phys. Rev. Lett. **94**, 184503 (2005).
[14] C.-Y. Chen and L.-W. Lo, Magnetohydrodynamics **42**, 31 (2006); J. Magn. Magn. Mater. **305**, 440 (2006).
[15] C. Lorenz and M. Zahn, Phys. Fluids **15**, S4 (2003).
[16] S. Rhodes, J. Perez, S. Elborai, S.-H Lee, and M. Zahn, J. Magn. Magn. Mater. **289**, 353 (2005).
[17] S. Elborai, D.-K. Kim, X. He, S.-H Lee, S. Rhodes, and M. Zahn, J. Appl. Phys. **97**, 10Q303 (2005).
[18] M. Zahn and R. E. Rosensweig, IEEE Trans. Magn. **16**, 275 (1980).
[19] J. A. Miranda, Phys. Rev. E **62**, 2985 (2000).
[20] D. P. Jackson and J. A. Miranda, Phys. Rev. E **67**, 017301 (2003).
[21] J. A. Miranda and R. M. Oliveira, Phys. Rev. E **69**, 066312 (2004).
[22] R. M. Oliveira and J. A. Miranda, Phys. Rev. E **73**, 036309 (2006).
[23] M. M. Maiorov and A. O. Tsebers, Magnetohydrodynamics (N.Y.) **19**, 376 (1983).
[24] A. Cebers, Magnetohydrodynamics (N.Y.) **33**, 48 (1997).
[25] M. Igonin and A. Cebers, Phys. Fluids **15**, 1734 (2003).
[26] C.-Y. Chen and C.-Y. Wen, J. Magn. Magn. Mater. **252**, 296 (2002).
[27] C.-Y. Chen, Phys. Fluids **15**, 1086 (2003).
[28] C.-Y. Chen, H.-J. Wu, and L. Hsu, J. Magn. Magn. Mater. **289**, 364 (2005).

[29] C.-Y. Chen and H.-J. Wu, J. Magn. Magn. Mater. **289**, 339 (2005).
[30] C.-Y. Chen and H.-J. Wu, Phys. Fluids **17**, 042101 (2005).
[31] D. Korteweg, Arch. Neerl. Sci. Exactes Nat., Ser. 3A **2**, 6 (1901).
[32] D. Joseph, Eur. J. Mech. B/Fluids **9**, 565 (1990).
[33] G. Galdi, D. Joseph, L. Prezisi, and S. Rionero, Eur. J. Mech. B/Fluids **10**, 565 (1991).
[34] H. Hu and D. Joseph, Z. Angew. Math. Phys. **43**, 626 (1992).
[35] D. Joseph, A. Huang, and H. Hu, Physica D **97**, 104 (1996).
[36] C.-Y. Chen, L. L. Wang, and E. Meiburg, Phys. Fluids **13**, 2447 (2001).
[37] C.-Y. Chen, C.-H. Chen, and J. A. Miranda, Phys. Rev. E **71**, 056304 (2005).
[38] B. A. Francis and R. G. Horn, J. Appl. Phys. **89**, 4167 (2001).
[39] D. Derks, A. Lindner, C. Creton, and D. Bonn, J. Appl. Phys. **93**, 1557 (2003).
[40] S. Poivet, F. Nallet, C. Gay, and P. Fabre, Europhys. Lett. **62**, 244 (2003).
[41] M. Tirumkudulu, W. B. Russel, and T. J. Huang, Phys. Fluids **15**, 1588 (2003).
[42] R. D. Welsh, M.Sc. thesis, Massachusetts Institute of Technology, 2001.
[43] J. A. Miranda, Phys. Rev. E **69**, 016311 (2004).
[44] J. A. Miranda, R. M. Oliveira, and D. P. Jackson, Phys. Rev. E **70**, 036311 (2004).
[45] S. Poivet, F. Nallet, C. Gay, J. Teisseire, and P. Fabre, Eur. Phys. J. E **15**, 97 (2004).
[46] A. Lindner, D. Derks, and M. J. Shelley, Phys. Fluids **17**, 072107 (2005).
[47] G. I. Taylor, Proc. R. Soc. London, Ser. A **219**, 186 (1953).
[48] C.-Y. Chen, C.-H. Chen, and J. A. Miranda, Phys. Rev. E **73**, 046306 (2006).
[49] I.-G. Chu, M.Sc. thesis, Da-Yeh University, Taiwan, 1998 (unpublished).
[50] C. T. Tan and G. M. Homsy, Phys. Fluids **31**, 1330 (1988).
[51] C.-Y. Chen and E. Meiburg, J. Fluid Mech. **371**, 233 (1998); **371**, 269 (1998).
[52] E. Meiburg and C.-Y. Chen, SPE J. **5**, 129 (2000).
[53] C.-Y. Chen and S. W. Wang, Fluid Dyn. Res. **30**, 315 (2002).
[54] M. Ruith and E. Meiburg, J. Fluid Mech. **420**, 225 (2000).
[55] F. Gazeau, E. Dubois, J.-C. Bacri, F. Boué, A. Cebers, and R. Perzynski, Phys. Rev. E **65**, 031403 (2002).
[56] D. P. Jackson and J. A. Miranda (unpublished).
[57] S. K. Thamida, P. V. Takhistov, and H.-C. Chang, Phys. Fluids **13**, 2190 (2001).